



A new magnetic bio-sorbent for arsenate removal from the contaminated water: Characterization, isotherms, and kinetics

Laleh Adlnasab^{1*}, Nader Djafarzadeh², Akram Maghsodi¹

¹Department of Chemistry, Chemistry and Petrochemistry Research Center, Standard Research Institute, Karaj, Iran

²Department of Chemistry, School of Science, Islamic Azad University, Miyaneh Branch, Miyaneh, Iran

Abstract

Background: Arsenic (AS) is a heavy metal pollutant in water that has been known as one of the most important environmental contaminants due to its serious effects on both human health and the environment. This study was conducted to investigate the efficiency of calcined Co/Fe/Al LDH@Fe₃O₄@PA as a new magnetic bio-sorbent for AS removal from the polluted water.

Methods: At first, magnetic ternary calcined layered double hydroxide (Co/Fe/Al LDH) was synthesized through co-precipitation procedure. The synthesized CLDH was modified with phenylalanine amino acid, named CLDH@Fe₃O₄@PA. Infrared spectroscopy, X-ray diffraction, transmission, and field emission scanning electron microscopy (FESEM) were used to confirm the synthesis of the sorbent. The removal time, pH, and the sorbent dose were studied and optimized as the effective parameters on the As (V) removal.

Results: The XRD, FTIR, TEM, SEM, EDS, and VSM techniques confirmed the properties of the synthesized magnetic bio-sorbent. Based on the optimization study, pH=6, the sorbent concentration of 30 mg, and the removal time of 5 minutes were considered as the optimum conditions with about 91% AS removal. The Langmuir isotherm with higher R² value was matched well with the obtained results, and values obtained for q_m and R_L were 167 mg g⁻¹ and 0.976 to 0.993, respectively. The kinetics studies were fitted well with the linear pseudo-first-order model with higher R² at sorption process.

Conclusion: The real samples results confirmed the excellent As (V) sorption capacity of the synthesized magnetic bio-sorbent in comparison with other sorbents. Therefore, CLDH@Fe₃O₄@PA sorbent is introduced as a new suitable sorbent for removal of As (V) from the polluted water.

Keywords: Water pollution, Phenylalanine, Ferrosferic oxide, Arsenic

Citation: Adlnasab L, Djafarzadeh N, Maghsodi A. A new magnetic bio-sorbent for arsenate removal from the contaminated water: characterization, isotherms, and kinetics. Environmental Health Engineering and Management Journal 2020; 7(1): 49–58. doi: 10.34172/EHEM.2020.07.

Article History:

Received: 28 September 2019

Accepted: 23 February 2020

ePublished: 10 March 2020

*Correspondence to:

Laleh Adlnasab

Email:

laleh_adlnasab@yahoo.com

Introduction

Arsenic (As) is a heavy metal present in the ecosystem, particularly in the groundwater in the forms of arsenite (As (III)) and arsenate (As (V)). As (III) is more mobile and toxic, therefore, its removal from water is not easy (1,2). AS is observed in the wastewater of the industrial emissions, mining industry, combustion of fossil fuels, agricultural pesticides and herbicides. Water contamination with AS is a serious global environmental challenge threatening some countries, such as the USA, China, Canada, Mexico, Argentina, Bangladesh, India, and etc. The long-term use of AS-polluted water may lead to some types of serious diseases and cancers. For this reason, the World Health Organization (WHO) has determined the value of 10 µg L⁻¹ as the acceptable concentration of AS in drinking water (3). Therefore, different procedures, such as ion exchange, adsorption, precipitation, and membrane techniques have

been studied for AS removal from aqueous solutions, among which, adsorption technique is more popular and practical, cost-effective, easy to use, which has a good efficiency (1-3). Different adsorbents have been studied for As removal, such as hydroxides and oxides of iron(III) (1,3-5), hydroxides and oxides of aluminum (1,6), activated carbon (7), chitosan (8,9), activated alumina (10), zinc oxide (1,11), biosorbent (9,12), layered double hydroxides (LDH_s) (13-19), and magnetic Fe₃O₄-graphene (20). LDHs are known as inorganic compounds which have a structure similar to clays. LDHs have wide applications in the adsorption/separation or removal, electrochemistry, optical, medical, drug or gene carriers, catalysis, and composite materials (18,21,22). The structure of LDHs is based on the brucite-like layers with positive charge in the sheets and negative charge in the interlayer spaces.

In the interlayer spaces, different types of organic/



inorganic anions can be interchanged with the present anions. Thus, they can be used as good ion-exchangers and adsorbents (21,22). These materials have large surface area, desirable thermal stability, low cost, and high anion exchange capacity, attracting the attention of researchers as a proper sorbent for removing heavy metals including AS, lead, selenium, cadmium, copper, chromium, zinc, and antimonate from aqueous solutions (13,17,23,24). Furthermore, LDHs have been used as a sublayer to place nanoparticles, such as Fe_3O_4 , silver, graphene, and TiO_2 in order to increase the function of materials (17,18).

The separation and recycling of nano-scaled LDHs as a sorbent from liquid phases is very difficult. However, with the creation of magnetic properties (Fe_3O_4 nanoparticles) in these materials, they can be separated easily from the aqueous solutions using a strong magnet (17,25). In fact, the magnetic property can remove the need for long centrifuge step, thus, it saves time.

The adsorption or removal of different materials or ions by LDHs has been studied. Huang et al modified an LDH with EDTA and bamboo biomass for Cr^{+6} removal from aqueous solutions (26). Asiabi et al prepared different LDHs modified with the diphenylamine-4-sulfonate for the highly selective removal of the heavy metals. Also, they synthesized an Ni/Al LDH intercalated with zwitterionic glycine for the removal of As, Cr, and Se (27). Hu and O'Hare recommended the synthesis of belt-like Mg-Al LDHs modified using tri-block copolymers (28). Xu et al synthesized hierarchical flower-like glycerol-modified $\text{Mg}_2\text{Al}-\text{Cl}$ LDH microspheres for adsorbing methyl orange (29). In addition, the modified $\text{Fe}_3\text{O}_4@ \text{MCM}@\text{Cu}-\text{Fe}-\text{LDH}$ nanoparticles was synthesized for the removal of alizarin yellow in our previous study (30). LDHs have been reported as AS sorbents in some studies (13,15-19,31-34).

Recently, biosorbents with more compatibility have been studied and some biological materials, such as drug molecules, vitamins, peptides, and porphyrins have been intercalated to LDHs layers (24,32,33). As an interesting group of amino acids, biomaterials have amine ($-\text{NH}_2$) and carboxyl ($-\text{COOH}$) functional groups, enabling them to link to the LDHs layers. In fact, the intercalation of amino acids into the layers of LDHs changes the properties of LDHs. Since, some amino acids and AS acids have possible similarity, arsenate or arsenite ions in aqueous solutions can be exchanged with amino acid molecules (13,16,24). However, the intercalation of LDHs with phenylalanine has not been reported up to now.

The aim of this study was to synthesize a magnetic ternary calcined Co/Fe/Al layered double hydroxide (CLDH@ Fe_3O_4), via the co-precipitation method and intercalated with phenylalanine amino acid (PA) as a magnetic biosorbent. The surface morphology, the crystalline and the chemical structure of the sorbent were characterized using Fourier-transform infrared (FTIR), X-ray diffraction (XRD), field emission scanning electron microscopy

(FESEM), transmission electron microscopy (TEM), energy-dispersive x-ray spectroscopy (EDX), and element mapping. The effective parameters in As (V) removal were evaluated.

Materials and Methods

$\text{FeCl}_3 \cdot 6\text{H}_2\text{O}$, $\text{FeCl}_2 \cdot 4\text{H}_2\text{O}$, $\text{CoCl}_2 \cdot 6\text{H}_2\text{O}$, $\text{Al}(\text{NO}_3)_3 \cdot 9\text{H}_2\text{O}$, sodium hydroxide (NaOH), L-phenylalanine amino acid (PA), ammonia solution (25% wt), toluene, ethanol (96%), n-propanol, and toluene (C_7H_8) were purchased from Merck (Darmstadt, Germany). AS standard solution (1000 ppm) and tetraethyl orthosilicate (TEOS) were purchased from Sigma-Aldrich (St. Louis, MO, USA). The As (V) standard stock solution (100 mg L^{-1}) was prepared by diluting AS standard solution.

Synthesis of calcined Co/Fe/Al layered double hydroxide nanoparticles

Ternary Co/Fe/Al LDH sorbent was synthesized using co-precipitation method (16). Firstly, NaOH solution (1 mol L^{-1}) was added very slowly to 20 mL deionized water until pH reached 9.5. Then, 1.23 g (0.13 mol) $\text{CoCl}_2 \cdot 6\text{H}_2\text{O}$, 1.03 g (0.13 mol) $\text{FeCl}_2 \cdot 4\text{H}_2\text{O}$, and 1.95 g (0.13 mol) $\text{Al}(\text{NO}_3)_3$ were dissolved in 40 mL deionized water and added drop by drop into the solution under intense stirring. The pH of solution was held at 9.5–10.0 by drop-wise increasing the NaOH solution (1 mol L^{-1}) at 80°C . Then, the obtained slurry was refluxed in a round-bottom flask at 70°C under vigorous stirring for 1 h. The obtained slurry was aged at 70°C for 24 h. Finally, the obtained precipitate (Co/Fe/Al LDH) was centrifuged and washed with the deionized water until pH of the solution reached 7. The synthesized LDH was dried at 50°C for 12 h and calcination was performed at 500°C for 3 h by furnace in air atmosphere, leading to an increase in the porosity of the Co/Fe/Al LDH (35). The calcined material was signed as CLDH.

Synthesis of $\text{Fe}_3\text{O}_4@ \text{SiO}_2$

Fe_3O_4 nanoparticles were synthesized by the in-situ chemical co-precipitation method (34). Briefly, $\text{FeCl}_2 \cdot 4\text{H}_2\text{O}$ and $\text{FeCl}_3 \cdot 6\text{H}_2\text{O}$ were dissolved in the deionized water. Afterwards, ammonia was added and heated at 80°C for 1 h. The magnetic Fe_3O_4 nanoparticles were washed and covered with a thin layer of SiO_2 microspheres by the sol-gel procedure. In brief, 17 mL TEOS was added drop-wise to the mixed solution of deionized water and n-propanol at ratio 1:2 and also Fe_3O_4 nanoparticles at 38°C under argon atmosphere and intense stirring at 38°C for 17 h. Finally, after being washed with deionized water and ethanol, $\text{Fe}_3\text{O}_4@ \text{SiO}_2$ nanoparticles were dried at 75°C .

Synthesis of CLDH@ Fe_3O_4

To prepare CLDH@ Fe_3O_4 nanoparticles, both synthesized CLDH (2 g) and $\text{Fe}_3\text{O}_4@ \text{SiO}_2$ (1 g) were added into 50 mL mixed solution of toluene and ethanol (1.5:1 v/v) and ultrasonicated for 30 min. Then, the suspension was

stirred at 70°C for 24 h. Afterwards, the CLDH@Fe₃O₄ was filtered and washed with deionized water and dried at 40°C overnight.

Modification of CLDH@Fe₃O₄ with Phenylalanine

At first, 0.2 g phenylalanine was dissolved in pre-boiled and cooled deionized water and the solution pH was adjusted at 9.5-10 by NaOH solution (1 mol L⁻¹). Then, the synthesized CLDH@Fe₃O₄ was dispersed in 50 mL deionized water at 70°C and added drop-wise to the phenylalanine solution. The mixture was refluxed at 70°C for 24 h. Afterwards, the obtained CLDH@Fe₃O₄@PA was washed with the deionized water and dried at 50°C.

Arsenic removal tests

Effective parameters including pH, sorbent dosage, and removal time were studied for the removal of AS. For this purpose, 20 mg of CLDH@Fe₃O₄@PA sorbent was added into 25 mL of As (V) standard solution and sonicated for 5 minutes. Then, the separation of the sorbent from the solution was performed by a magnet and the residual As (V) value in the solution was obtained using polarography method. Finally, the As (V) removal percentage (R%) was calculated using Eq. (1).

$$R\% = \frac{C_0 - C_e}{C_0} \times 100 \quad (1)$$

where, C₀ and C_e (mg L⁻¹) are the As (V) ions initial and residual concentrations in the solution, respectively.

Instruments

The As (V) removal measurements were carried out using a polarography apparatus (884 Professional VA, Metrohm: Swiss). The morphology and particle size of the synthesized sorbent were analyzed by a transmission electron spectroscopy (TEM, Philips, CM 120, Netherlands) and a field emission scanning electron microscopy (FESEM, VEGA3, TESCAN, Czech Republic). The pH measurements were performed using a digital pH meter (Mettler Toledo, M225, Switzerland). The chemical composition of the biosorbent was specified by an energy dispersive X-ray spectroscopy (SIRIUS SD, scientific instrument, the United Kingdom). The synthesized sorbent was characterized by the X-ray diffraction over the 2θ ranging from 10 to 80° using Cu K_α radiation technique (X'Pert PRO MPD, PANalytical Company, Netherlands, λ = 1.54060 Å). The magnetic properties of synthesized sorbent were investigated by a vibrating-sample magnetometer (VSM) (AGFM/VSM 3886 Kashan, Iran) in the range of -8000 to 8000 Oe at room temperature. The FTIR spectra of the sorbent were recorded by the Bruker Vertex 70 in the frequency range of 400-4000 cm⁻¹. An ultrasonic bath (50/60 Hz, 350W) was applied for dispersing the materials in solutions (Euronda, Eurosonic 4D, 320 V, Italy).

Results

Structural study

FTIR studies

The FTIR spectra of Co/Fe/Al LDH, CLDH, Fe₃O₄@SiO₂, CLDH@Fe₃O₄, Phenylalanine, and CLDH@Fe₃O₄@PA samples shown in Figure 1 (a-f) were in the range of 400-4000 cm⁻¹.

The Co/Fe/Al LDH FTIR spectrum is presented in Figure 1a. The broad peak at about 3430 cm⁻¹ was ascribed to the O-H groups stretching vibration, which was connected to the interlayer water molecules in the brucite-like layers. Also, the bending vibration of interlayer water molecules (H-O-H) was observed at 1673 cm⁻¹ (13,16,17). The hydroxide groups belonged to the synthesized LDH and water molecules present in the interlayer. The peaks in the region of 500-800 cm⁻¹ were ascribed to the stretching vibration of metal-oxygen bonds, Co-O, Al-O, and Fe-O (13,16,17). In addition, the mentioned peaks was observed in the calcined LDH sample (Figure 1b), but their intensity decreased.

The wide band in Figure 1c at 3450 cm⁻¹ was attributed to the stretching vibration of absorbed O-H group on Fe₃O₄ nanoparticles. As shown in Figure 1, this peak was observed at all spectra, showing a number of O-H groups was present on the samples surface. The broad peak in Figure 1c at about 1100 cm⁻¹ was ascribed to the stretching vibration of Si-O-Si groups, which were located on the Fe₃O₄ nanoparticles surface and observed in the FTIR spectrum of CLDH@Fe₃O₄ (Figure 1d). In addition, the peaks at 590 and 640 cm⁻¹ were ascribed to the vibration of Fe-O bond in Fe₃O₄ nanoparticles, which was present in the spectra of samples including Fe₃O₄.

In Figure 1d, all mentioned peaks for CLDH (Figure 1b) and Fe₃O₄@SiO₂ (Figure 1c) were observed for the synthesized CLDH@Fe₃O₄. The FTIR spectra of L-phenylalanine amino acid are demonstrated in Figure 1e. The sharp peak at about 3200 cm⁻¹ was related to asymmetric NH stretching and the stretching vibration of COO⁻ occurring at 1480 cm⁻¹, confirming the existence of amine and carboxyl groups in phenylalanine. The bands at 3050 and 2908 cm⁻¹ confirmed the stretching vibration of CH and CH₂ groups. Also, the stretching vibration of C=C was seen at 2080 cm⁻¹. The bands at 1490 and 1450 cm⁻¹ indicated corroborated the anti-symmetric and symmetric stretching of C=O functional group. The stretching vibration of C-C bond was appeared at 1120 and 1193 cm⁻¹. The vibration of benzene ring occurred at about 706 cm⁻¹. Furthermore, the peak at 1045 cm⁻¹ confirmed the stretching vibration of C-N group in phenylalanine. The peaks at 880 and 564 cm⁻¹ were related to the substituted aromatic ring distribution (36,37).

Finally, the FTIR spectra for CLDH@Fe₃O₄@PA sorbent and all peaks mentioned for CLDH@Fe₃O₄ and phenylalanine amino acid samples are presented in Figure 1f.

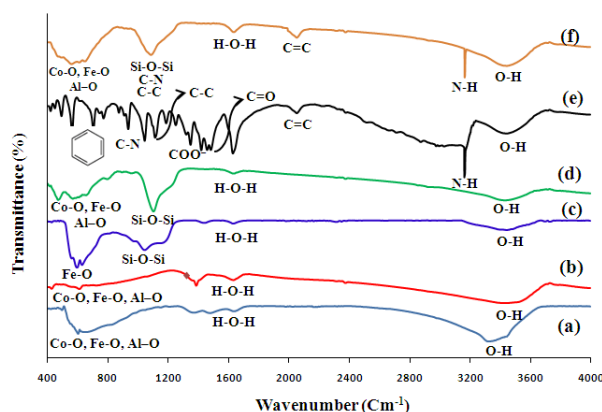


Figure 1. FTIR spectra of the synthesized (a) Co/Fe/Al LDH, (b) C-LDH, (c) $\text{Fe}_3\text{O}_4@\text{SiO}_2$, (d) $\text{CLDH}@\text{Fe}_3\text{O}_4$, (e) Phenylalanine, and (f) $\text{CLDH}@\text{Fe}_3\text{O}_4@\text{PA}$ samples.

X-ray diffraction studies

The XRD patterns of ternary LDH, $\text{Fe}_3\text{O}_4@\text{SiO}_2$, and $\text{CLDH}@\text{Fe}_3\text{O}_4$ are presented in Figure 2 (a-c). The specified diffraction peaks corresponding to the hydrotalcite structure of Co/Fe/Al LDHs (Figure 2a) are observed at $2\theta=11.6^\circ$ (003), 23° (006), 34° (012), 38° (015), 45° (018), 59° (110), and 62° (113) (16).

Magnetic Fe_3O_4 nanoparticles indicated diffraction peaks (Figure 2b) with 2θ of about 18° (111), 32° (220), 36° (311), 44° (400), 54° (422), 58° (511), and 64° (440) as the specified peaks of the Fe_3O_4 , which are matched well with the XRD pattern of the standard Fe_3O_4 nanoparticles in literature (JCPDS card No. 74-0748).

In Figure 2c, the XRD pattern of synthesized $\text{CLDH}@\text{Fe}_3\text{O}_4$ is recorded, all observed peaks for $\text{Fe}_3\text{O}_4@\text{SiO}_2$ and Co/Fe/Al LDH samples are presented, and the formation of $\text{CLDH}@\text{Fe}_3\text{O}_4$ sorbent is approved.

Also, VSM analysis was done to confirm the magnetic properties of the synthesized sorbent with a field between -8000 and 8000 Oe at room temperature, and the results are shown in Figure 3.

TEM, FESEM, and EDS studies

The surface morphology, elemental analysis, and

dispersion of elements in the synthesized sorbent were investigated using TEM and FESEM images, EDS, and mapping images. The TEM images of the $\text{CLDH}@\text{Fe}_3\text{O}_4@\text{PA}$ are demonstrated in Figure 4. It was found that the nanosheets of LDH and Fe_3O_4 nanoparticles of the sample were in the plate- and spherical-like shapes, respectively. According to the TEM images, the average length of the LDH nanosheets and their thickness were approximately 35 and 10 nm, respectively.

In addition, the FESEM images of Co/Fe/Al LDH (Figure 5a) and $\text{CLDH}@\text{Fe}_3\text{O}_4$ (Figure 5b) nanoparticles are presented in Figure 5. Co/Fe/Al LDH had a layered structure and the presence of magnetic Fe_3O_4 nanoparticles caused the agglomeration of LDH nanoparticles on the sorbent (Figure 5b). The EDS spectra of the nanosorbent are displayed in Figure 5c. The existence of Fe (8.14 A%), Co (8.32 A%), Al (14.11 A%), Si (1.13 A%), and O (68.3 A%) elements was confirmed by the EDS analysis in the nanosorbent structure (Figure 5c). Moreover, the obtained results of EDS mapping image are shown in Figure 5d, indicating that all mentioned elements were distributed in a very regular and uniform pattern in the nanosorbent (Figure 5d).

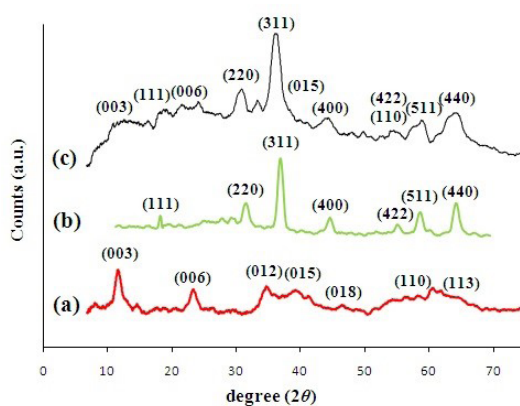


Figure 2. XRD patterns of the synthesized (a) Co/Fe/Al LDH, (b) $\text{Fe}_3\text{O}_4@\text{SiO}_2$, and (c) $\text{CLDH}@\text{Fe}_3\text{O}_4$ samples.

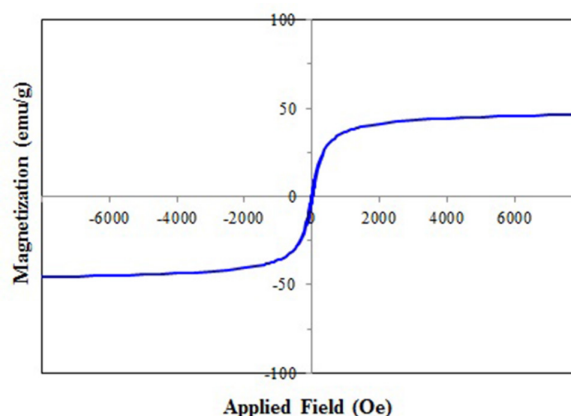


Figure 3. VSM analysis of the synthesized sorbent.

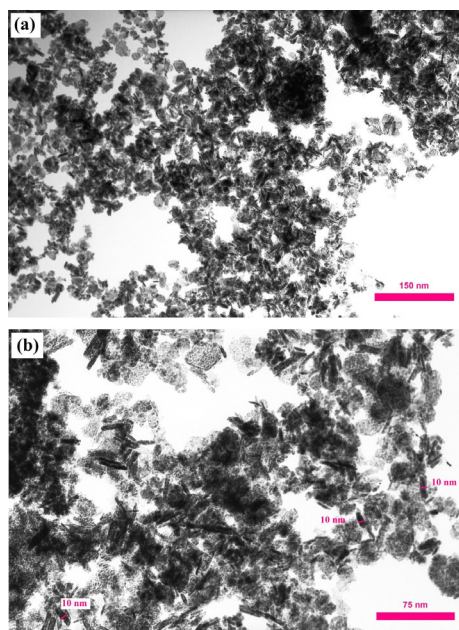


Figure 4. TEM images of the synthesized CLDH@Fe₃O₄@PA sorbent: (a) low magnification, (b) high magnification.

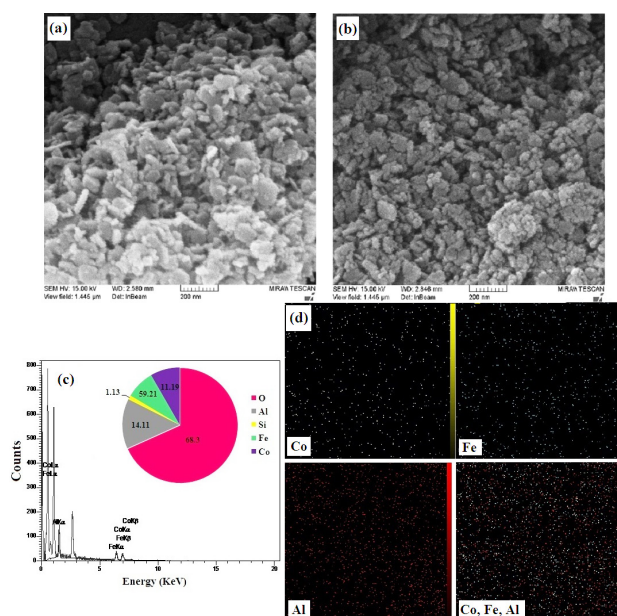


Figure 5. FESEM images of the synthesized (a) Co/Fe/Al LDH, (b) CLDH@Fe₃O₄ samples, (C) EDS analysis for CLDH@Fe₃O₄ sample, and (d) images of element mapping analysis of Co, Fe, and Al in Co/Fe/Al LDH sample.

Discussion

Optimization of removal conditions

In order to gain the maximum removal yield, pH of the solution, the sorbent concentration, and sorption time as the effective parameters in removal experiments were investigated and optimized. In all experiments, 25 mL aqueous standard solutions of AS with a concentration of 60 $\mu\text{g L}^{-1}$ were applied.

Generally, the solution pH is one of the important

parameters, which affects the AS adsorption by influencing the adsorption efficiency. Actually, the pH of solution can affect both ionic or molecular forms of the analyte (the AS species) and the sorbent surface charge (zeta potential of the sorbent).

To investigate the effect of pH on the AS sorption by the CLDH@Fe₃O₄@PA sorbent, various pH values from 2.0 to 12.0 were tested. NaOH or HCl solutions were used to adjust the pH of solution. Figure 6a demonstrated the effect of pH on the As (V) removal in the aqueous solution. According to Figure 6a, the As (V) removal percentage increased with increasing pH from 2.0 to 6.0, then, it was decreased. So, the optimum pH was found to be 6.0, since the removal percentage reached the maximum level at this pH value, given the fact that at acidic pH, LDH and Fe₃O₄@SiO₂ were dissolved and the structure of sorbent was destroyed. In addition, in the solution with higher pHs, the hydroxide precipitate of As (V) ions was formed and competition between OH⁻ and As (V) ions for the adsorption on the surface of the sorbent occurred (15,38). Considering the pH-dependent behavior of AS adsorption on the synthesized sorbent, the adsorption process seemed to be controlled by different factors, such as electrostatic interactions and surface adsorption.

Studies have shown that LDH is stable at pH between 6 and 10 (39). When pH arises, LDH decomposes to M(OH)₂, and subsequently, to MO where M is a metal (40). At pH lower than 4, the dissolution of LDHs occurs (41). The thermal decomposition of LDH takes place at 150°C in the solution and at 250°C at a solid state in air (40). At higher temperatures, thermal decomposition takes place. According to literature, the corresponding LDH stabilities are in the order Mg < Mn < Co < Ni < Zn for M(II) and Al < Fe for M(III) (42).

In order to realize the adsorption mechanism, the pH of zero-point charge (pH_{PZC}) of the synthesized CLDH@Fe₃O₄@PA sorbent was determined (Figure 6b). The electrical charge density on the surface of the sorbent at pH_{PZC} was zero. The pH_{PZC} of the synthesized sorbent was 7.25, lower than the pH_{PZC}. The surface of the sorbent had a positive charge, while over this amount (pH > 7.25), the surface of the sorbent had a negative charge. Arsenate (As (V)) species have different forms in the different solutions with different pHs including H₃AsO₄ (pH < 2), H₂AsO₄⁻ (pH: 2-7), HAsO₄²⁻ (pH: 7-11), and AsO₄³⁻ (pH > 12) (43). When pH increased from 2.0 to 6.0, the number of H₂AsO₄⁻ ions increased and the surface of the sorbent carried a positive charge (pH < pH_{PZC}), thus, it could absorb the arsenate anions due to attractive electrostatic effects, finally, resulting in higher removal percentage in comparison to lower pH values. In addition, the structure of the synthesized sorbent was destroyed at lower pH values, leading to low removal percentage of arsenate. However, the removal percentage enhanced with an increase in the pH up to 6. The removal percentage was decreased at pH values higher than 6, which is attributed

to the neutral and negative surface charge of the sorbent. Therefore, the mechanism of arsenate adsorption on the synthesized magnetic bio-sorbent was based on the electrostatic interactions.

At $\text{pH} > 6$, the surface of the sorbent was negatively charged and the concentration of HAsO_4^{2-} in the solution increased. So, there was no interaction between arsenate and sorbent. The results showed that the removal percentage of arsenate decreased with increasing the solution pH. Finally, $\text{pH} 6.0$ was selected as the optimum pH with the removal percentage of 91% for arsenate species.

The effect of sorbent concentration on the removal percentage of arsenate was studied using 10-70 mg sorbent. The obtained results are presented in Figure 6c. As can be seen in this figure, the removal percentage increased from 60 to 89%, when the sorbent concentration increased from 10 to 30 mg, probably because of the increase in the accessible sites and the sorbent surface area. There was no considerable changes in the removal percentage of arsenate by increasing the sorbent dose (more than 30 mg). In fact, there was an equilibrium state between arsenate adsorption and desorption (44). Thus, the optimum concentration of the sorbent was 30 mg for the subsequent experiments.

The removal time is another effective factor in the adsorption experiments, which depends on the interaction between the analyte and the sorbent. In order to investigate the effect of removal time on the removal percentage of AS by the synthesized $\text{CLDH}@Fe_3O_4@PA$ sorbent, removal times between 1.0 and 25.0 minutes with other experimental conditions were selected as the optimum values. The associated results are shown in Figure 6d. Actually, As (V) removal percentage increased with increasing the removal time, and then, reached the maximum value at 5 minutes. Then, the removal percentage remained constant with increasing time, which could be justified by this fact that at times over 5 minutes, saturation stage was created and based on the equilibration process, arsenate desorption/adsorption repeated again and the removal percentage remained constant. Based on the results, the time of 5.0 minutes was considered as the optimum removal time.

Adsorption isotherm

Adsorption isotherm was applied to explain the interaction between the sorbent and analyte. The adsorption isotherm models, such as Langmuir and Freundlich isotherms were used for fitting the adsorption equilibrium data of As (V) on the synthesized sorbent. In the Langmuir isotherm, the monolayer adsorption happens on the specific sites of the sorbent surface, which are the same and tantamount. Furthermore, the homogeneity of the adsorption is expressed by the Langmuir isotherm, meaning that the activation energy and adsorption enthalpy are constant

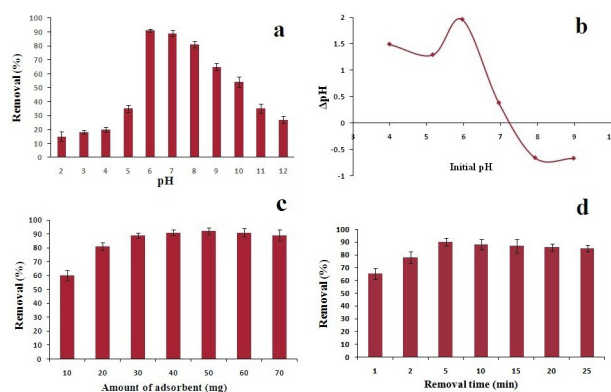


Figure 6. (a) The effect of pH on As (V) removal by $\text{CLDH}@Fe_3O_4@PA$ sorbent, (b) pH_{PZC} of synthesized magnetic bio-sorbent, (c) the effect of sorbent value, and (d) removal time on the As (V) removal by $\text{CLDH}@Fe_3O_4@PA$ sorbent.

for each molecule. The linear and non-linear forms of the Langmuir model are shown as the following equations (Eqs. 2 and 3) (45):

$$\frac{C_e}{q_e} = \frac{C_e}{q_{\max}} + \frac{1}{K_L q_{\max}} \text{ (linear)} \quad (2)$$

$$q_e = \frac{K_L q_{\max} C_e}{1 + K_L C_e} \text{ (non-linear)} \quad (3)$$

where, K_L is the Langmuir isotherm constant related to the binding affinity points and the strength of adsorption (L mg^{-1}), C_e is the equilibrium concentration in the aqueous solution (mg L^{-1}), q_{\max} is the maximum adsorption capacity (mg g^{-1}), and q_e is the equilibrium adsorption capacity (mg g^{-1}). The q_{\max} and K_L values were obtained from the slope and intercept of plot of C_e/q_e versus C_e , respectively, (Figure 7), and the results are presented in Table 1. Also, a parameter named separation factor (R_L) could be predicted as the favorability ($0 < R_L < 1$) or unfavorability ($R_L > 1$) of an adsorption system. This factor is calculated according to Eq. 4 (30,46):

$$R_L = \frac{1}{1 + K_L C_0} \quad (4)$$

Where, C_0 is the various initial As (V) concentrations and the calculated R_L values ranged 0.976 to 0.993, and the results indicated that the adsorption process was favorable. The Freundlich isotherm expresses that the surface of sorbent is heterogeneous and the adsorption sites do not have the same energy distribution. Also, Freundlich model is useful for the amorphous surfaces (30). The linear and non-linear forms of Freundlich isotherm are presented using Eqs. 5 and 6 (47):

$$\log q_e = + \frac{1}{n} \log C_e + \log K_F \text{ (linear)} \quad (5)$$

$$q_e = K_F C_e^{1/n} \text{ (non-linear)} \quad (6)$$

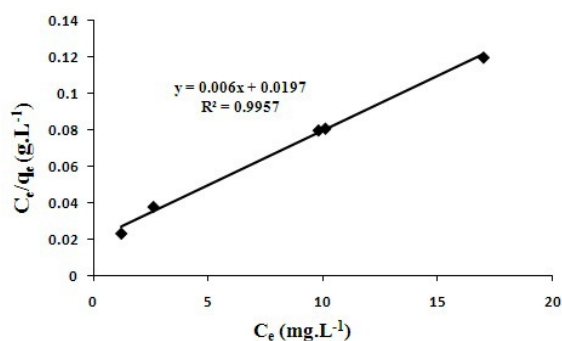


Figure 7. Linear plots of Langmuir model for As (V) removal by the synthesized magnetic bio-sorbent at 25°C.

where K_F and n are the Freundlich constants, which give the information about the maximum adsorption capacity (mg g^{-1}) and surface heterogeneity, respectively. If the $1/n$ value gets closer to zero (between 0 and 1), it shows that the heterogeneity of surface increases ($n > 1$). Also, the adsorption process is chemisorption if $1/n > 1$ ($n < 1$) (45). In other words, the adsorption would be favorable if $1 < n < 10$. The values of n (2.49) and K_F (46.80) were calculated from the plot slope and intercept of $\log q_e$ versus $\log C_e$ (linear model), respectively. However, the Langmuir q_{max} and K_F value of Freundlich isotherm for the As (V) removal by $\text{CLDH@Fe}_3\text{O}_4\text{/PA}$ nanosorbent were 167 and 46.8 mg g^{-1} , respectively. The Langmuir R^2 values (linear $R^2 = 0.9957$ and non-linear $R^2 = 0.8780$) were higher in comparison with Freundlich model (linear $R^2 = 0.9605$ and non-linear $R^2 = 0.9436$) (Table 1), indicating that the Langmuir model was fitted well with experimental data rather than Freundlich model for desirable As (V) removal by the synthesized nanosorbent.

The results of comparison of q_m , R^2 , and K_L for the linear and non-linear forms of Langmuir isotherm showed that the linear form of Langmuir isotherm was the appropriate isotherm for the As (V) adsorption on the surface of $\text{CLDH@Fe}_3\text{O}_4\text{/PA}$ nanosorbent. The R^2 values and other isotherm parameters are presented in Table 1.

Adsorption kinetics

In this study, kinetics tests were performed by sonicating the synthesized magnetic bio-sorbent (30 mg) into 25 mL As (V) standard solution ($60 \mu\text{g L}^{-1}$) at the optimum pH of 6 and removal time in the range of 5 to 25 minutes at 25°C. The pseudo-first-order and pseudo-second-order kinetic models were applied to explain the adsorption kinetics of As (V) on $\text{CLDH@Fe}_3\text{O}_4\text{/PA}$ sorbent (48). The linear form of this model is presented as Eq. 7:

Table 1. Parameters of different isotherms for the As (V) removal on $\text{CLDH@Fe}_3\text{O}_4\text{/PA}$ sorbent

Isotherms	Parameters		R^2
Langmuir (linear)	q_m (mg g^{-1})	167	0.9957
	K_L (L mg^{-1})	0.304	
	R_L range	0.976-0.993	
Langmuir (Non-linear)	q_m (mg g^{-1})	174.9	0.8780
	K_L (L mg^{-1})	0.244	
	$1/n$	0.401	
Freundlich (linear)	n	2.494	0.9605
	K_F (mg g^{-1})	46.80	
	$1/n$	0.436	
Freundlich (Non-linear)	n	2.29	0.9436
	K_F (mg g^{-1})	43.62	

$$\log(q_e - q_t) = \log q_e - \frac{K_1}{2.303} t \quad (7)$$

where K_1 is the rate constant of the pseudo-first-order model, q_t is the sorbent adsorption capacity (mg g^{-1}) at time t (min), and q_e is the adsorption capacity of the sorbent at equilibrium time (mg g^{-1}). The slope and intercept of the linear plot of $\log(q_e - q_t)$ versus time (Figure 8a) is used for the calculation of the K_1 value and estimated q_e (from the curve).

Also, the pseudo-second-order model was applied for analyzing the kinetic behavior in the adsorption process and its linear form is obtained using Eq. 8 (49):

$$\frac{t}{q_t} = \frac{1}{K_2 q_e^2} + \frac{1}{q_e} t \quad (8)$$

where K_2 is the rate constant of the pseudo-second-order adsorption model ($\text{g mg}^{-1} \text{min}^{-1}$).

The obtained R^2 values for the pseudo-first-order (Figure 8a) and pseudo-second-order model (Figure 8b) were 0.9768 and 0.95, respectively. According to the kinetics parameters and R^2 values presented in Table 2, the experimental data were matched well with the linear pseudo-first-order model and described the kinetic of adsorption process logically.

Analysis of real samples

To evaluate the matrix effects on the As (V) removal, the tap water of Karaj, Iran, was used as the real sample and

Table 2. The parameters of the pseudo-first-order and pseudo-second-order kinetic for removal of As (V) by $\text{CLDH@Fe}_3\text{O}_4\text{/PA}$ sorbent

Temperature (°C)	Lagergren pseudo-first-order kinetics			Pseudo-second-order kinetics		
	q_e (mg g^{-1})	K_1 ($\text{g mg}^{-1} \text{min}^{-1}$)	R^2	q_e (mg g^{-1})	K_2 ($\text{g mg}^{-1} \text{min}^{-1}$)	R^2
25	72.5	0.07	0.9768	5.2	0.036	0.95

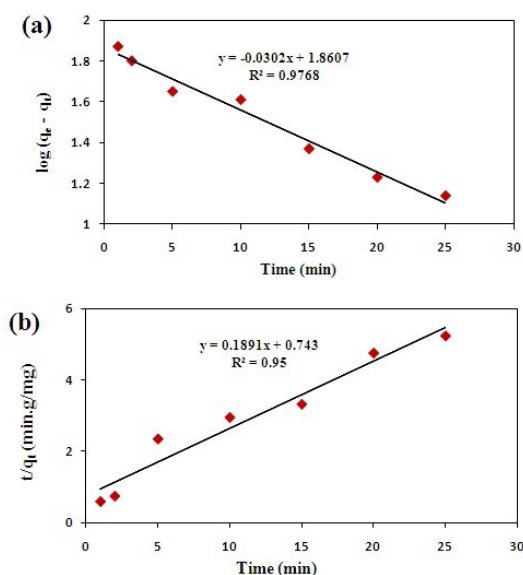


Figure 8. Linear plots of (a) pseudo-first-order kinetic and (b) pseudo-second-order kinetic.

spiked with various concentrations of As (V) standard solution. The final As (V) concentrations in water samples are presented in Table 3. After removal at the optimum conditions, the residual As (V) values were determined and the removal percentage was calculated (Table 3). The removal percentages for three samples ranged from 87.5 to 95%. The results obtained from the three replicate tests on the real samples demonstrated that the synthesized sorbent can be used as an appropriate sorbent for As (V) removal from the contaminated water. So, the selectivity of the synthesized adsorbent was investigated to calculate the As removal in the presence of Pb(II), Cd(II), and Fe (II). The selectivity experiments showed that the synthesized adsorbent had high selectivity for As removal.

Comparison of CLDH@Fe₃O₄@PA sorbent with other sorbents for As (V) removal

The performance of CLDH@Fe₃O₄@PA sorbent in comparison with other sorbents for As (V) removal is listed in Table 4. The obtained results demonstrated that the synthesized sorbent had a significant performance for As (V) removal in comparison to other sorbents. Therefore, CLDH@Fe₃O₄@PA sorbent can be introduced as a new suitable sorbent for removal of As (V) from the polluted water.

Conclusion

In this study, the AS removal from the contaminated water using CLDH@Fe₃O₄@PA as a new magnetic bio-sorbent was investigated. The effective parameters on the AS removal were explored and optimized. According to the results, under optimum conditions (pH= 6, sorbent dose= 30 mg, and removal time= 5 minutes), the AS removal

Table 3. Analysis of the spiked real samples with different concentrations of As (V) (n=3)

Sample	C _{initial} (mg.L ⁻¹)	C _{final} (mg.L ⁻¹)	Removal (%)	RSD% (n=3)
1	0.02	0.001	95	4.64
2	0.04	0.0034	91.5	4.57
3	0.06	0.0075	87.5	4.42

Table 4. Comparative evaluation of different adsorbents with CLDH@Fe₃O₄@PA sorbent for As (V) removal

Adsorbent	q _{max} (mg.g ⁻¹)	Ref
Mesoporous alumina and Fe-doped alumina	62	(10)
Starch modified Mg/Al LDH	5.987	(15)
Magnetic LDH nanocomposites	82.31	(16)
Mg-Fe-Ala-LDH	23.6	(17)
Mg-Al-NO ₃ LDH (Mg/Al = 4)	76.92	(19)
Chitosan-magnetic-graphene oxide nanocomposite	45	(20)
CLDH@Fe ₃ O ₄ @PA	167	This study

percentage was about 91%. In addition, the adsorption behavior of AS on the synthesized sorbent was investigated by the Langmuir and Freundlich isotherms. The results obtained were matched well with the Langmuir isotherm, so that the values for q_m and R_L were obtained to be 167 mg g⁻¹ and 0.976 to 0.993, respectively, indicating that the As (V) adsorption on the sorbent surface was desirable. Furthermore, the real sample analysis showed that the synthesized sorbent could remove As (V) ions from the contaminated water. In fact, this sorbent exhibited fast, cost-effective, and easy As (V) removal from the AS-contaminated water.

Acknowledgements

The authors would like to gratitude the Standard Research Institute (Karaj, Iran), Iran National Science Foundation (INSE, project No: 94811616), and Miyaneh Branch of Islamic Azad University that supported this study.

Ethical issues

The authors hereby certify that all data collected during the research are as expressed in the manuscript, and no data from the study has been or will be published elsewhere separately.

Competing interests

The authors have declared that they have no conflict of interests.

Authors' contributions

All authors contributed to the data collection, analysis, and interpretation. All authors reviewed, refined, and approved the manuscript.

References

- Lata S, Samadder SR. Removal of arsenic from water using nano adsorbents and challenges: a review. *J Environ Manage* 2016; 166: 387-406. doi: 10.1016/j.jenvman.2015.10.039.
- Jadhav SV, Bringas E, Yadav GD, Rathod VK, Ortiz I, Marathe KV. Arsenic and fluoride contaminated groundwaters: a review of current technologies for contaminants removal. *J Environ Manage* 2015; 162: 306-25. doi: 10.1016/j.jenvman.2015.07.020.
- Hao L, Zheng T, Jiang J, Zhang G, Wang P. Removal of As(III) and As(V) from water using iron doped amino functionalized sawdust: characterization, adsorptive performance and UF membrane separation. *Chem Eng J* 2016; 292: 163-73. doi: 10.1016/j.cej.2016.01.097.
- Sahu UK, Sahu MK, Mahapatra SS, Patel RK. Removal of As(III) from aqueous solution using Fe₃O₄ nanoparticles: process modeling and optimization using statistical design. *Water Air Soil Pollut* 2017; 228(1): 45. doi: 10.1007/s11270-016-3224-1.
- Suresh Kumar P, Flores RQ, Sjöstedt C, Önnby L. Arsenic adsorption by iron-aluminium hydroxide coated onto macroporous supports: Insights from X-ray absorption spectroscopy and comparison with granular ferric hydroxides. *J Hazard Mater* 2016; 302: 166-74. doi: 10.1016/j.jhazmat.2015.09.065.
- Tchieda VK, D'Amato E, Chiavola A, Parisi M, Chianese A, Amamra M, et al. Removal of arsenic by alumina: effects of material size, additives, and water contaminants. *Clean (Weinh)* 2016; 44(5): 496-505. doi: 10.1002/clen.201400599.
- Deliyanni EA, Kyzas GZ, Triantafyllidis KS, Matis KA. Activated carbons for the removal of heavy metal ions: a systematic review of recent literature focused on lead and arsenic ions. *Open Chem* 2015; 13(1): 699-708. doi: 10.1515/chem-2015-0087.
- Pontoni L, Fabbicino M. Use of chitosan and chitosan-derivatives to remove arsenic from aqueous solutions--a mini review. *Carbohydr Res* 2012; 356: 86-92. doi: 10.1016/j.carres.2012.03.042.
- Rahim M, Mas Haris MRH. Application of biopolymer composites in arsenic removal from aqueous medium: a review. *J Radiat Res Appl Sci* 2015; 8(2): 255-63. doi: 10.1016/j.jrras.2015.03.001.
- Inchaurredo N, di Luca C, Mori F, Pintar A, Žerjav G, Valiente M, et al. Synthesis and adsorption behavior of mesoporous alumina and Fe-doped alumina for the removal of dominant arsenic species in contaminated waters. *J Environ Chem Eng* 2019; 7(1): 102901. doi: 10.1016/j.jece.2019.102901.
- Singh N, Singh SP, Gupta V, Yadav HK, Ahuja T, Tripathy SS, et al. A process for the selective removal of arsenic from contaminated water using acetate functionalized zinc oxide nanomaterials. *Environ Prog Sustain Energy* 2013; 32(4): 1023-9. doi: 10.1002/ep.11698.
- Boddu VM, Abburi K, Talbott JL, Smith ED, Haasch R. Removal of arsenic (III) and arsenic (V) from aqueous medium using chitosan-coated biosorbent. *Water Res* 2008; 42(3): 633-42. doi: 10.1016/j.watres.2007.08.014.
- Asiabi H, Yamini Y, Shamsaye M. Highly selective and efficient removal of arsenic(V), chromium(VI) and selenium(VI) oxyanions by layered double hydroxide intercalated with zwitterionic glycine. *J Hazard Mater* 2017; 339: 239-47. doi: 10.1016/j.jhazmat.2017.06.042.
- Iqbal MA, Asghar H, Iqbal MA, Fedel M. Sorption of As(V) from aqueous solution using in situ growth MgAl-NO₃ layered double hydroxide thin film developed on AA6082. *SN Appl Sci* 2019; 1(7): 666. doi: 10.1007/s42452-019-0669-z.
- Duan S, Ma W, Cheng Z, Zong P, Sha X, Meng F. Preparation of modified Mg/Al layered double hydroxide in saccharide system and its application to remove As(V) from glucose solution. *Colloids Surf A Physicochem Eng Asp* 2016; 490: 250-7. doi: 10.1016/j.colsurfa.2015.11.060.
- Hong J, Zhu Z, Lu H, Qiu Y. Synthesis and arsenic adsorption performances of ferric-based layered double hydroxide with α -alanine intercalation. *Chem Eng J* 2014; 252: 267-74. doi: 10.1016/j.cej.2014.05.019.
- Lee SH, Choi H, Kim KW. Removal of As(V) and Sb(V) in water using magnetic nanoparticle-supported layered double hydroxide nanocomposites. *Journal of Geochemical Exploration* 2018; 184: 247-54. doi: 10.1016/j.gexplo.2016.11.015.
- Daud M, Kamal MS, Shehzad F, Al-Harhi MA. Graphene/layered double hydroxides nanocomposites: a review of recent progress in synthesis and applications. *Carbon* 2016; 104: 241-52. doi: 10.1016/j.carbon.2016.03.057.
- Rahman MT, Kameda T, Kumagai S, Yoshioka T. Adsorption isotherms and kinetics of arsenic removal from aqueous solution by Mg-Al layered double hydroxide intercalated with nitrate ions. *Reaction Kinetics, Mechanisms and Catalysis* 2017; 120(2): 703-14. doi: 10.1007/s11144-016-1116-4.
- Sherlala AIA, Raman AAA, Bello MM, Buthiyappan A. Adsorption of arsenic using chitosan magnetic graphene oxide nanocomposite. *J Environ Manage* 2019; 246: 547-56. doi: 10.1016/j.jenvman.2019.05.117.
- Daniel S, Thomas S. Layered double hydroxides: fundamentals to applications. 1- Layered Double Hydroxide Polymer Nanocomposites. *Woodhead Publishing Series in Composites Science and Engineering* 2020; 1-76. doi: 10.1016/B978-0-08-101903-0.00001-5.
- Wang X, Lin Y, Su Y, Zhang B, Li C, Wang H, et al. Design and synthesis of ternary-component layered double hydroxides for high-performance supercapacitors: understanding the role of trivalent metal ions. *Electrochim Acta* 2017; 225: 263-71. doi: 10.1016/j.electacta.2016.12.160.
- Yang F, Sun S, Chen X, Chang Y, Zha F, Lei Z. Mg-Al layered double hydroxides modified clay adsorbents for efficient removal of Pb²⁺, Cu²⁺ and Ni²⁺ from water. *Appl Clay Sci* 2016; 123: 134-40. doi: 10.1016/j.clay.2016.01.026.
- Zhang X, Yan L, Li J, Yu H. Adsorption of heavy metals by l-cysteine intercalated layered double hydroxide: kinetic, isothermal and mechanistic studies. *J Colloid Interface Sci* 2020; 562: 149-58. doi: 10.1016/j.jcis.2019.12.028.
- Alinezhad H, Amiri A, Tarahomi M, Maleki B. Magnetic solid-phase extraction of non-steroidal anti-inflammatory drugs from environmental water samples using polyamidoamine dendrimer functionalized with magnetite nanoparticles as a sorbent. *Talanta* 2018; 183: 149-57. doi: 10.1016/j.talanta.2018.02.069.
- Huang D, Liu C, Zhang C, Deng R, Wang R, Xue W, et al. Cr(VI) removal from aqueous solution using biochar modified with Mg/Al-layered double hydroxide intercalated

- with ethylenediaminetetraacetic acid. *Bioresour Technol* 2019; 276: 127-32. doi: 10.1016/j.biortech.2018.12.114.
27. Asiabi H, Yamini Y, Shamsaye M, Tahmasebi E. Highly selective and efficient removal and extraction of heavy metals by layered double hydroxides intercalated with the diphenylamine-4-sulfonate: a comparative study. *Chem Eng J* 2017; 323: 212-23. doi: 10.1016/j.cej.2017.04.096.
 28. Hu G, O'Hare D. Unique layered double hydroxide morphologies using reverse microemulsion synthesis. *J Am Chem Soc* 2005; 127(50): 17808-13. doi: 10.1021/ja0549392.
 29. Xu J, Deng H, Song J, Zhao J, Zhang L, Hou W. Synthesis of hierarchical flower-like Mg₂Al-Cl layered double hydroxide in a surfactant-free reverse microemulsion. *J Colloid Interface Sci* 2017; 505: 816-23. doi: 10.1016/j.jcis.2017.06.080.
 30. Adlnasab L, Shabaniyan M, Ezoddin M, Maghsodi A. Amine rich functionalized mesoporous silica for the effective removal of alizarin yellow and phenol red dyes from waste waters based on response surface methodology. *Mater Sci Eng B* 2017; 226: 188-98. doi: 10.1016/j.mseb.2017.09.017.
 31. Koilraj P, Takaki Y, Sasaki K. Adsorption characteristics of arsenate on colloidal nanosheets of layered double hydroxide. *Appl Clay Sci* 2016; 134(P2): 110-9. doi: 10.1016/j.clay.2016.06.002.
 32. Khan AI, O'Hare D. Intercalation chemistry of layered double hydroxides: recent developments and applications. *J Mater Chem* 2002; 12(11): 3191-8. doi: 10.1039/B204076J.
 33. Bessaies H, Iftekhar S, Doshi B, Kheriji J, Ncibi MC, Srivastava V, et al. Synthesis of novel adsorbent by intercalation of biopolymer in LDH for the removal of arsenic from synthetic and natural water. *J Environ Sci* 2020; 91: 246-61. doi: 10.1016/j.jes.2020.01.028.
 34. Maghsodi A, Adlnasab L, Shabaniyan M, Javanbakht M. Optimization of effective parameters in the synthesis of nanopore anodic aluminum oxide membrane and arsenic removal by prepared magnetic iron oxide nanoparticles in anodic aluminum oxide membrane via ultrasonic-hydrothermal method. *Ultrason Sonochem* 2018; 48: 441-52. doi: 10.1016/j.ultsonch.2018.07.003.
 35. dos Santos RMM, Gonçalves R, Constantino VRL, Santilli CV, Borges PD, Tronto J, et al. Adsorption of Acid Yellow 42 dye on calcined layered double hydroxide: effect of time, concentration, pH and temperature. *Appl Clay Sci* 2017; 140: 132-9. doi: 10.1016/j.clay.2017.02.005.
 36. Mahalakshmi R, Jesuraja SX, Das SJ. Growth and characterization of L-phenylalanine. *Cryst Res Technol* 2006; 41(8): 780-3. doi: 10.1002/crat.200510668.
 37. Caroline ML, Vasudevan S. Growth and characterization of L-phenylalanine nitric acid, a new organic nonlinear optical material. *Mater Lett* 2009; 63(1): 41-4. doi: 10.1016/j.matlet.2008.08.059.
 38. Babae S, Daneshfar A, Khezeli T. Determination of carboxylic acids in non-alcoholic beer samples by an ultrasonic-assisted dispersive micro-solid phase extraction based on Ni/Cu-Al layered double hydroxide nanocomposites followed by gas chromatography. *Ultrason Sonochem* 2017; 34: 847-55. doi: 10.1016/j.ultsonch.2016.07.023.
 39. Rives V. *Layered Double Hydroxides: Present and Future*. New York: Nova Publishers; 2001.
 40. Britto S, Radha AV, Ravishankar N, Vishnu Kamath P. Solution decomposition of the layered double hydroxide (LDH) of Zn with Al. *Solid State Sci* 2007; 9(3-4): 279-86. doi: 10.1016/j.solidstatesciences.2007.01.002.
 41. Tang S, Lee HK. Application of dissolvable layered double hydroxides as sorbent in dispersive solid-phase extraction and extraction by co-precipitation for the determination of aromatic acid anions. *Anal Chem* 2013; 85(15): 7426-33. doi: 10.1021/ac4013573.
 42. Bocclair JW, Braterman PS. Layered double hydroxide stability. 1. Relative stabilities of layered double hydroxides and their simple counterparts. *Chem Mater* 1999; 11(2): 298-302. doi: 10.1021/cm980523u.
 43. Guo X, Chen F. Removal of arsenic by bead cellulose loaded with iron oxyhydroxide from groundwater. *Environ Sci Technol* 2005; 39(17): 6808-18. doi: 10.1021/es048080k.
 44. Zhou Q, Lei M, Li J, Zhao K, Liu Y. Determination of 1-naphthol and 2-naphthol from environmental waters by magnetic solid phase extraction with Fe@MgAl-layered double hydroxides nanoparticles as the adsorbents prior to high performance liquid chromatography. *J Chromatogr A* 2016; 1441: 1-7. doi: 10.1016/j.chroma.2016.02.061.
 45. Ilgen O, Dulger HS. Removal of oleic acid from sunflower oil on zeolite 13X: kinetics, equilibrium and thermodynamic studies. *Ind Crops Prod* 2016; 81: 66-71. doi: 10.1016/j.indcrop.2015.11.050.
 46. Duan S, Tang R, Xue Z, Zhang X, Zhao Y, Zhang W, et al. Effective removal of Pb(II) using magnetic Co_{0.6}Fe_{2.4}O₄ micro-particles as the adsorbent: synthesis and study on the kinetic and thermodynamic behaviors for its adsorption. *Colloids Surf A Physicochem Eng Asp* 2015; 469: 211-23. doi: 10.1016/j.colsurfa.2015.01.029.
 47. Ghitescu RE, Volf I, Carausu C, Bühlmann AM, Gilca IA, Popa VI. Optimization of ultrasound-assisted extraction of polyphenols from spruce wood bark. *Ultrason Sonochem* 2015; 22: 535-41. doi: 10.1016/j.ultsonch.2014.07.013.
 48. Maran JP, Nivetha CV, Priya B, Al-Dhabi NA, Ponmurugan K, Manoj JJ. Modeling of polysaccharide extraction from *Gossypium arboreum* L. seed using central composite rotatable design. *Int J Biol Macromol* 2016; 86: 857-64. doi: 10.1016/j.ijbiomac.2016.01.094.
 49. Zhang Y, Lin X, Zhou Q, Luo X. Fluoride adsorption from aqueous solution by magnetic core-shell Fe₃O₄@alginate-La particles fabricated via electro-coextrusion. *Appl Surf Sci* 2016; 389: 34-45. doi: 10.1016/j.apsusc.2016.07.08